

Original Article

Antioxidant effect of bamboo leaves on the reproduction and embryonic development-related gene expression in mouse embryonic stem cells

Feng Yu¹, Xiaowei Qian¹, Zhanghui Zeng¹, Xiaoli Zhao¹, Rong Hou², Zhihe Zhang², Hongwu Bian¹, Ning Han¹, Junhui Wang¹, Muyuan Zhu¹

¹Key Laboratory for Cell and Gene Engineering of Zhejiang Province, College of Life Sciences, Zhejiang University, Hangzhou, China; ²The Key Laboratory for Conservation Biology of Endangered Wildlife, Chengdu, Sichuan Province, China

Received October 4, 2016; Accepted June 25, 2017; Epub August 15, 2017; Published August 30, 2017

Abstract: This study aims to investigate the effects of different concentrations of antioxidant of bamboo leaves (AOB) on mouse embryonic stem (mES) cells and to explore the underlying molecular mechanism by which AOB affects the proliferation and apoptosis of mES cells. Compared with the control group, Oct4 expression was remarkably upregulated and Nanog expression was downregulated in mES cells after treatment with AOB at 50 µg/ml, while both the expressions of Oct4 and Nanog were significantly upregulated in mES cells after treatment with AOB at 100 µg/ml. AOB exposure remarkably increased the level of p-ERK ($P < 0.01$), whereas treatment with ERK pathway inhibitor U0126 markedly depressed the level of p-ERK in AOB-treated embryoid bodies (mEBs) ($P < 0.01$). Moreover, the levels of β -catenin, SOX17, CABYR, and P450scc were significantly increased following AOB treatment, but decreased in the treatment with AOB+U0126 or AOB+DKK1 (Wnt pathway inhibitor) ($P < 0.01$). In conclusion, our data indicated that AOB had embryo-toxicity which might be mediated by activation of ERK and Wnt pathway.

Keywords: Antioxidant of bamboo leaves (AOB), mouse embryonic stem (mES), embryoid bodies (EBs), proliferation, apoptosis, reproduction, signaling pathway

Introduction

Antioxidant of bamboo leaves (AOB) is obtained from sorts of bamboo leaves. AOB has been reported recently, due to its antioxidative activity [1]. However, its dose-dependent toxicity and impact on animal reproduction and development remain unclear. The working principle of genechip technique is based on hybridization between target DNA/RNA extracted from cell lines or tissues and complementary short DNA-nucleotide oligomers grafted to the solid surface of the chip [2, 3]. Nowadays, genechip has been widely used in functional genomics and pathogenic mechanism exploration. Mouse embryonic stem (mES) cells, derived from the blastocyst stage early mammalian embryos, are distinguished by their ability to differentiate into any cell type and by their ability to propagate [4]. mES cell's properties include having a normal karyotype, maintaining high telomerase activity, and exhibiting remarkable long-term

proliferative potential [5]. It is now known that the feeder cells provide leukemia inhibitory factor (LIF) that is necessary to prevent ES cells from differentiation [6, 7]. However, these techniques have several drawbacks including the need for feeder-cells and/or use of undefined media containing animal derived components. When cultured in suspension without anti-differentiation factors, ES cells spontaneously differentiate and form three-dimensional multicellular aggregates called embryoid bodies (EBs) [8]. EBs recapitulate many aspects of cell differentiation during early embryogenesis, and play an important role in the differentiation of ES cells into a variety of cell types *in vitro* [9]. EBs is identified as the best models in the early embryo development and embryo toxicology research [10]. In this study, AOB-treatments were performed with mEBs derived from mES cells to investigate the effect of AOB on the expression of genes related to reproduction and embryonic development in mEBs.

Table 1. Primer sequences of real-time PCR

Gene	Sense (/Antisense)	T _m (°C)	Length (bp)
β-actin	GTGACGTTGACATCCGTAAAGA	60.3	245
	GCCGGACTCATCGTACTCC	61.6	
Oct4	AGAGGATCACCTTGGGGTACA	61.7	98
	CGAAGCGACAGATGGTGGTC	62.9	
Nanog	TTGCTTACAAGGGTCTGCTACT	60.4	106
	ACTGGTAGAAGAATCAGGGCT	60.1	
Nestin	CCCTGAAGTCGAGGAGCTG	60.9	114
	CTGCTGCACCTCTAAGCGA	61.7	
FGF5	GAAGCGTCTCACTCCCGAAG	62.3	93
	GAAGAAAACGTCGCGCTACT	60.7	
Brachyury	AGAGGATCACCTTGGGGTACA	61.7	98
	CGAAGCGACAGATGGTGGTC	62.9	
Flk1	CAAACCTCAATGTGTCTCTTTGC	60.2	97
	AGAGTAAAGCCTATCTCGCTGT	60.4	
AFP	CTTCCCTCATCCTCCTGCTAC	61.1	145
	ACAACTGGGTAAAGGTGATGG	60.2	
Sox17	CCAAAGCGGAGTCTCGCAT	62.4	125
	GCCTAGCATCTTGCTTAGCTC	60.6	
GATA6	TTGCTCCGGTAACAGCAGTG	62.4	105
	GTGGTCGCTTGTGTAGAAGGA	61.7	
SOX7	ATGCTGGGAAAGTCATGGAAG	60.0	201
	CGTGTCTGGTCACGAGAGA	61.2	
Camk2a	ACCTGCACCCGATTACAG	62.0	112
	TGGCAGCATACTCCTGACCA	62.8	
Pttg1	TCTGATCCGCTGTACTCTCCT	61.6	60
	AGGCGGCAATTCAACATCCA	62.5	
Smc1b	GAGAATTTCAAGTCGTGGCGA	60.6	193
	CAGGTTTTCCAGTATGTGCTCC	60.9	
ROCK2	TTGGTTCGTCATAAGGCATCAC	62.8	94
	TGTTGGCAAAGGCCATAATATCT	61.5	
SpMyb	GGTTGGGAGAATCGTGACTGC	63.0	299
	TAGACACACGTCGCCTCTTCA	62.9	
Wnt5a	ATGCAGTACATTGGAGAAGGTG	60.0	138
	CGTCTCTCGGCTGCCTATTT	61.7	
Star	TGCCCATCATTTTCATTCCTCT	60.3	232
	AAAAGCGGTTTCTCACTCTCC	60.2	
P450 _{scc}	TGGTGTCTTTATAGCCTCCTG	59.2	157
	CATCTCCTGTACCTCAAGTTGTG	59.3	

Materials and methods

Materials

mES cells: D3 mES cells were purchased from Institute of Biochemistry and Cell Biology, Shanghai Institutes for Biological Sciences,

Chinese Academy of Sciences. Mitomycin C and alkaline phosphatase ALP Kit were from Sigma. Leukemia inhibitory factor (LIF) was from Chemicon. Anti-Oct4 Rabbit IgG and fluorescence protection agent were from Abcam. Alexa488-conjugated; Goat anti-rabbit IgG was from Invitrogen. The primers were ordered from Shanghai Sangon Company.

Culture and identification of mES cells

A confluence of at least 90% for MEF feeder layer cells was used and the supernatant was aspirated. Fresh medium with 10 µg/ml mitomycin C was added to cells and incubated for 3 h at 37°C. After carefully removing the supernatant and washing with phosphate-buffered saline (PBS) 3-5 times, 1 ml of 0.05% trypsin/0.02% EDTA was added and incubated for 1-2 min. MEF cells were harvested by centrifuge at low-speed (300×g) for 5 min, and placed in flasks and incubated at 37°C with 5% CO₂. A total 1×10⁶ mES cells were harvested, placed on MEF feeder cells, and cultured at 37°C with 5% CO₂.

Alkaline phosphatase (ALP) assay

mES cells were washed three times with PBS and fixed with 1 ml citric acid-acetone-formaldehyde mixture for 45 s at room temperature (RT) [8]. After rinsing with deionized water, 1 ml alkaline dye mixture was added and cells were stained for 30 min at RT in the dark. mES cells were washed twice and ALP activity was determined under a microscope.

Immunofluorescence detection

mES cells were washed three times with PBS and fixed with 4% paraformaldehyde for 15 min at RT. After washing three times, PBS with 0.25% Triton X-100 was added and cells were incubated for 15 min at RT. After blocking for 30 min at RT, cells were incubated with the corresponding primary (overnight at 4°C), followed by secondary antibodies (1 h at RT in the dark) and fluorescence protective agent (30 min at RT). Finally, microscopic inspection and photo record were performed.

Preparation of mEBs

D3 mES cells at 80-90% were adopted for preparation of mEBs using differential adhesion

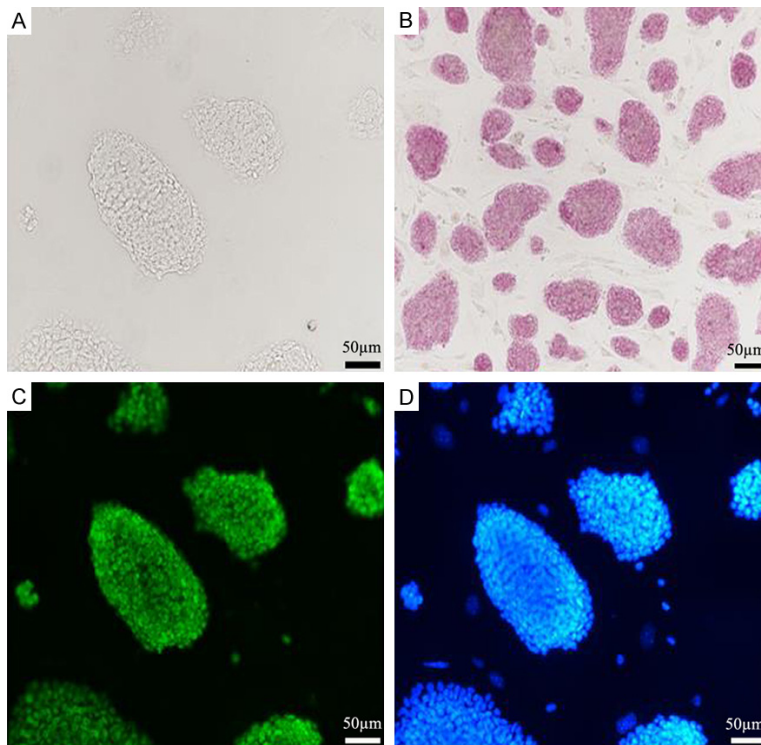


Figure 1. Pluripotency test of mES cells. A: Light microscope was used to check the state of mES cell colony; B: mES cells stained by ALP; C: mES cells' Oct4 immunohistochemistry; D: Dye the nuclear of mES cells.

method. mES cells were resuspended and adjusted to a density of 5×10^4 cells/ml. A total of 100 µl cells were seeded into sterile PCR microplates. Then the cells were spun down at 400 g for 5 min at 4°C. Cells were cultured at 37°C with 5% CO₂ for 48 h. Then mEBs were carefully transferred to a 6-well plate pre-coated with 0.1% gelatin, and incubated at 37°C with 5% CO₂ for 24 h. The medium was replaced every other day.

Real-time RT-PCR

Total RNAs were extracted from experimental groups (50 µg/ml and 100 µg/ml AOB-treated mEB cells) and purified respectively with the reagent kit following the manufacturer's instructions. One microgram of total RNA was reverse-transcribed to cDNA with random hexamer primers. β-actin was used as an internal control for gene expression normalization. Primers used are summarized in **Table 1**. PCR amplifications were performed using TAKARA master mix. For each PCR reaction, 1 µl template cDNA, equivalent to approximately 100 ng total RNA, was mixed with 12.5 µl 2× SYBR Green

PCR master mix and 0.4 µM forward and reverse primer in a final volume of 20 µl. The PCR conditions were as follows: initial enzyme activation at 95°C for 10 min, amplification for 40 cycles (95°C for 30 sec, 60°C for 60 sec), followed by a dissociation curve analysis.

Western blot analysis

Total proteins were extracted separately from experimental and control groups and quantified. The proteins were denatured, separated on sodium dodecylsulfate polyacrylamide gel electrophoresis (SDS-PAGE), and transferred to polyvinylidenedifluoride (PVDF) membrane. Membranes were blocked in Tris-Buffered Saline and Tween 20 (TBST) (150 mM NaCl, 10 mM Tris-HCl, pH 7.5 and 0.1% Tween 20) containing 5% (w/v) milk, and then

incubated with the corresponding primary and secondary antibodies. The primary antibodies used for this experiment were the rabbit anti-phosphorylated ERK (p-ERK), β-catenin, SOX17, CABYR, and P450scc. Goat anti-rabbit IgG was used as a secondary antibody and protein signals were detected using the ECL system.

Bioinformatics analysis

The functional annotation of differentially expressed genes was performed according to Gene Ontology databases [4]. The GO category was classified using hypergeometric distribution, and the Benjamini and Hochberg (BH) false discovery rate (FDR) algorithm was used to adjust the resulting *P* values. GO enrichment was considered to be significant if the FDR values were ≤ 0.05. Pathway analysis was used to identify the significant pathway of the differentially expressed genes according to Kyoto Encyclopedia of Genes and Genomes (KEGG). Similarly, hypergeometric distribution, followed by BH multiple testing correction, was performed to select the significant pathway, and the threshold of significance was defined as *P* value < 0.05.

The effect of AOB on mES

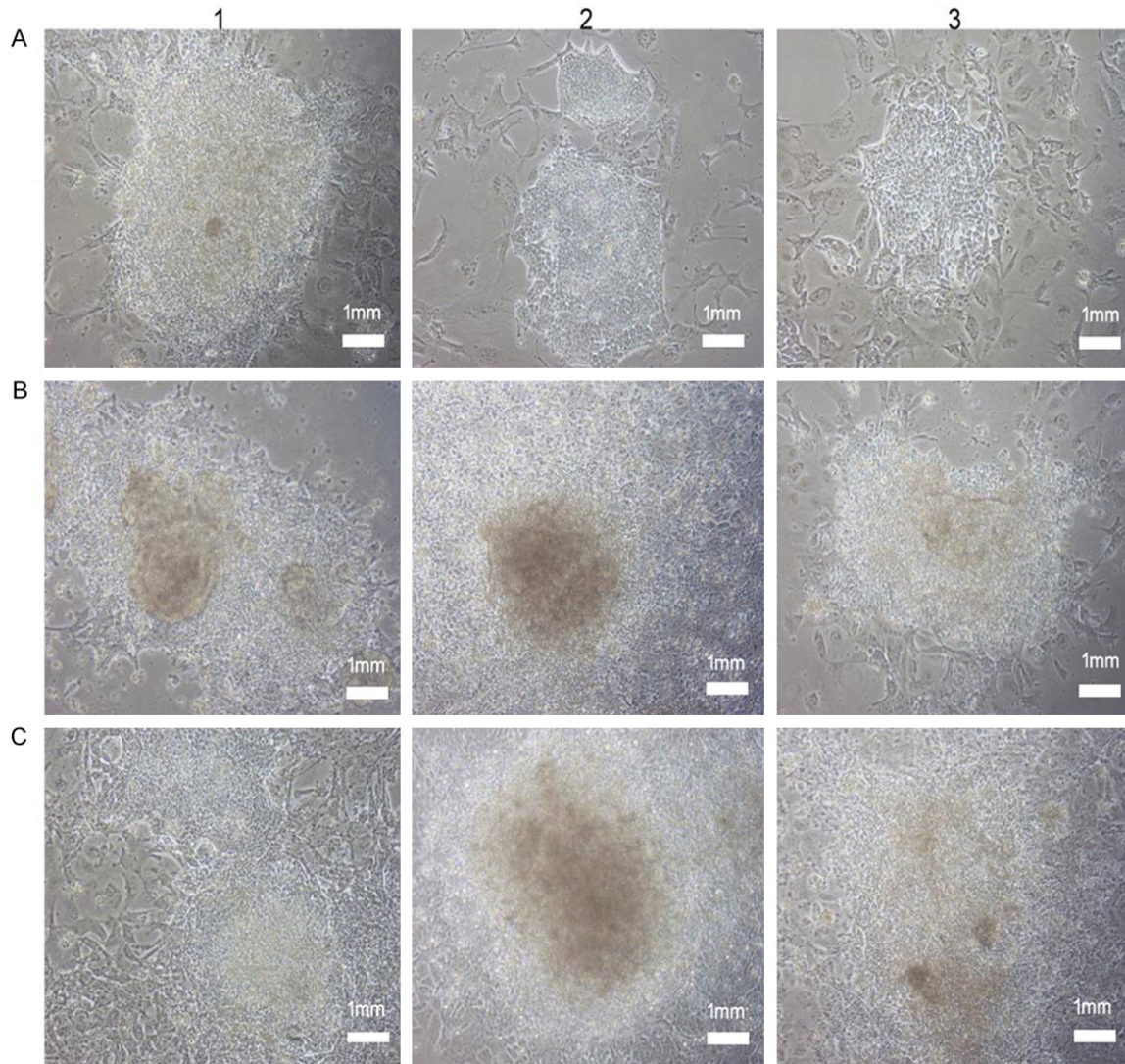


Figure 2. Effects of different AOB concentrations on mEBs formation ($\times 50$). The state of mEBs treated by AOB in different concentration was shown. 1: 0 $\mu\text{g/ml}$ AOB; 2: 50 $\mu\text{g/ml}$ AOB; 3: 100 $\mu\text{g/ml}$. A: mEBs cultured for 1 day; B: mEBs cultured for 4 days; C: mEBs cultured for 7 days.

Statistical analysis

All statistical analysis was performed using SPSS 20.0 (SPSS, Chicago, Illinois, USA). The data were expressed as the mean value \pm standard deviation (SD). Statistical analysis was performed by Student's t-test. Significance was considered as $P < 0.05$.

Results

Morphological observation and identification of mES cells

We observed that mES cells grew as colonies with clear edges, a large nuclei and dis-

tinct plasmosome. After staining with ALP, D3 cells were found to be strongly positive. Immunofluorescence cytochemistry showed high expression of Oct4 in D3 cells (**Figure 1**). The results suggested that mES cells were not differentiated, and were suitable for subsequent experiments.

Morphological observation of mEBs

To measure the cytotoxic effects of AOB on the mEBs, different concentrations of AOB were selected and applied to mEBs. As shown in **Figure 2**, lower concentrations of AOB, such as 50-100 $\mu\text{g/ml}$ could shrink the mEBs colonies

The effect of AOB on mES

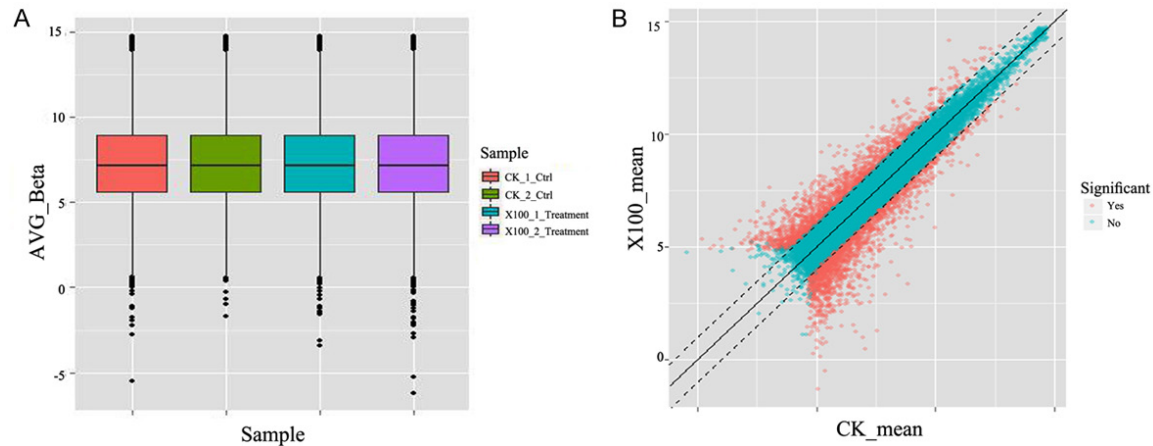


Figure 3. The analysis results of expression profiles of genechip in mEB 100 group. A: The Box Plot of data normalization, the minimum value; first quartile; median value; maximum value of four groups data (CK-1, 100-1; CK-2, 100-2); B: Cy2-Cy3 Scatter Plot of EB 100 $\mu\text{g}/\text{ml}$ group. X axis and Y axis is fluorescence signal of LogCy3 and LogCy5. The black solid line present diagonal line of 45 degree. Dashed present threshold of standard deviation. The dotted internal black dashed line present non-difference genes; The dotted outside black dashed line present difference genes; red color present significant difference genes; blue colored present non-significant difference genes.

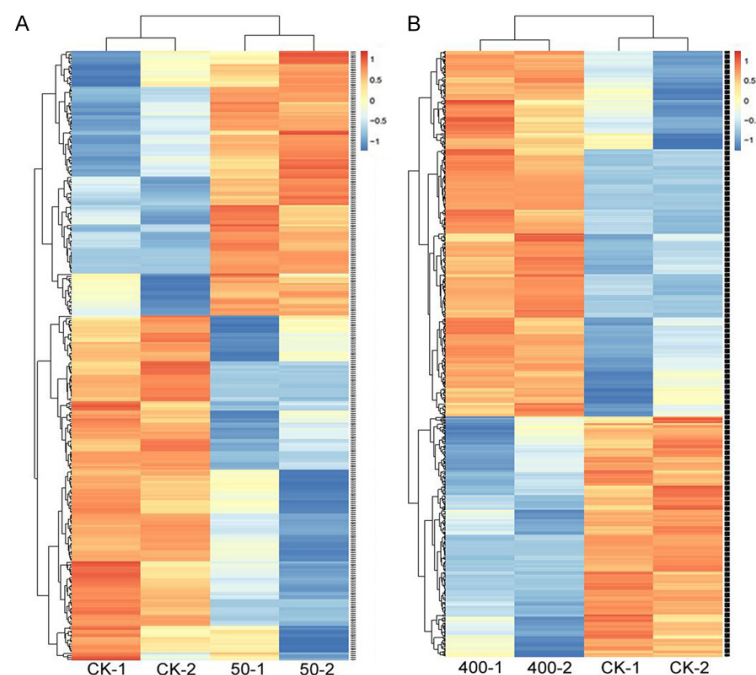


Figure 4. Cluster analysis of differentially expressed genes. A: 50 $\mu\text{g}/\text{ml}$ mEB group; B: 100 $\mu\text{g}/\text{ml}$ mEB group. Blue color present low expression genes, red color present high expression genes. Deep color indicates differentially expressed genes, and white color indicates no differences were found in gene expression.

but still maintained the morphology of mEBs. However, mEBs's extension was seriously inhibited and they started being dead and disrupted. These results indicated that the concentra-

tions of 50 and 100 $\mu\text{g}/\text{ml}$ of AOB were suitable for subsequent experiments.

Effects of AOB on gene expression of mEBs

A total of 683 differentially expressed genes were considered to be significant as fold change (FC) ≥ 1 and P value < 0.05 . Among these genes, 390 genes were up-regulated and 293 genes were down-regulated, as shown in **Figure 3**.

Hierarchical cluster analysis

Hierarchical cluster analysis was performed, which allows a rapid detection of alterations in gene expression and the identification of critical genes (**Figure 4**).

GO functional enrichment analysis

GO functional enrichment analysis were performed to seek differentially expressed genes between AOB-treated groups and control. As shown in **Figure 5**, differentially expressed

The effect of AOB on mES

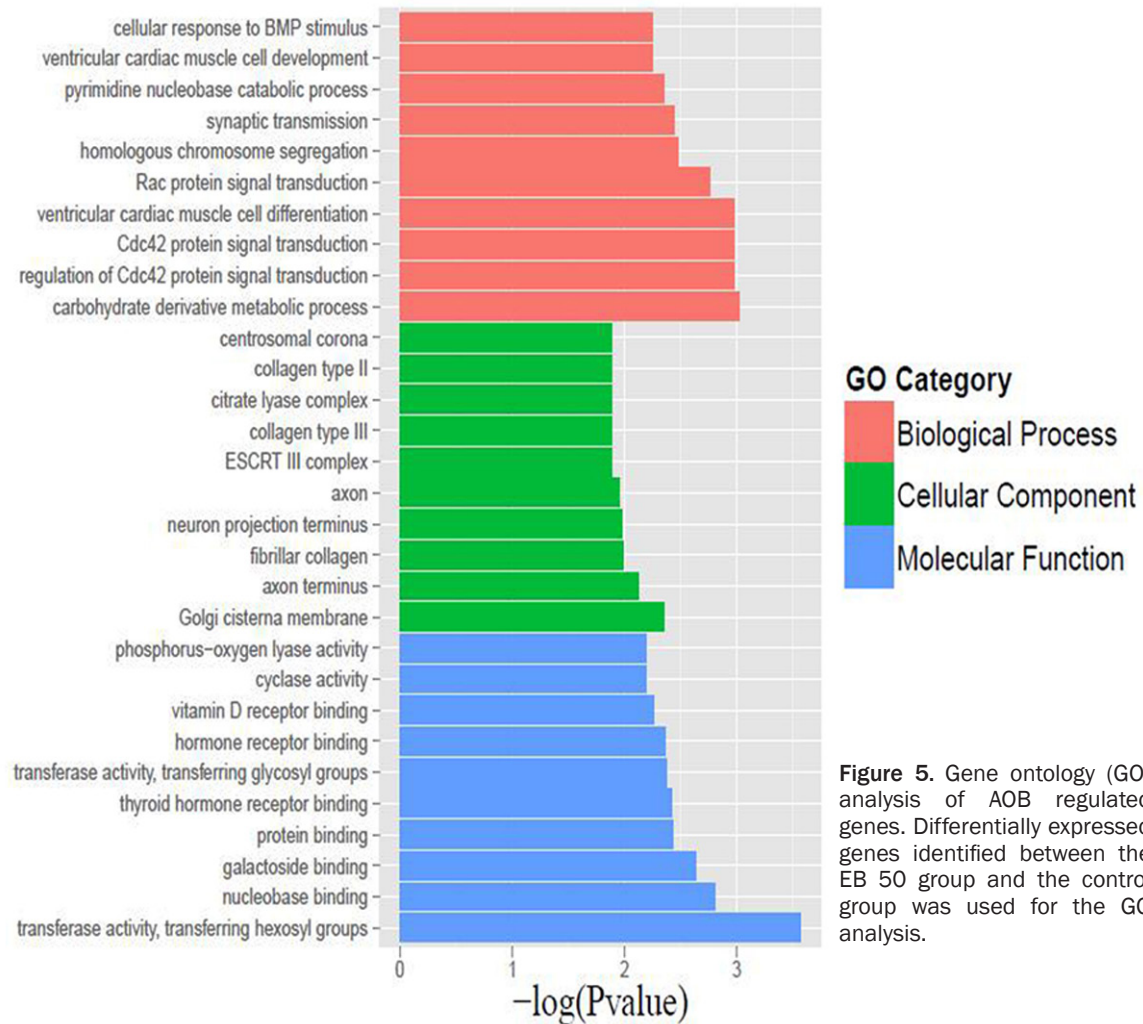


Figure 5. Gene ontology (GO) analysis of AOB regulated genes. Differentially expressed genes identified between the EB 50 group and the control group was used for the GO analysis.

genes in AOB-treated mEB cells were mainly associated with biological process, cellular constitution and molecular function.

KEGG pathway analysis

As shown in **Figure 6**, AOB-treatment of low concentration inhibited some signal pathways and activated others in mEBs. However, high concentration AOB had negative effect on all signaling pathways involved in our study. The results revealed that AOB was more toxic to mEBs at high concentration.

Effects of AOB on the expressions of stem cell marker genes

The expressions of Oct4 and Nanog were both upregulated significantly in 100 $\mu\text{g/ml}$ AOB-treated mEB cells (**Figure 7**). This result suggested that low concentration of AOB would

promote mES cell differentiation, but high concentration of AOB depressed mEB differentiation.

Different concentrations of AOB effect gene expressions

With 50 $\mu\text{g/ml}$ and 100 $\mu\text{g/ml}$ AOB treatments, the expressions of 25 genes were significantly changed in mEBs. Treatment with 100 $\mu\text{g/ml}$ AOB has higher effect on the gene expressions compared with that of 50 $\mu\text{g/ml}$ AOB (**Figure 8**). These results indicated that AOB influenced gene expressions of mEBs more effectively at high concentration.

Effects of AOB on the signal pathway of mEBs

As shown in **Figure 9**, compared with the control cells, treatment with AOB remarkably

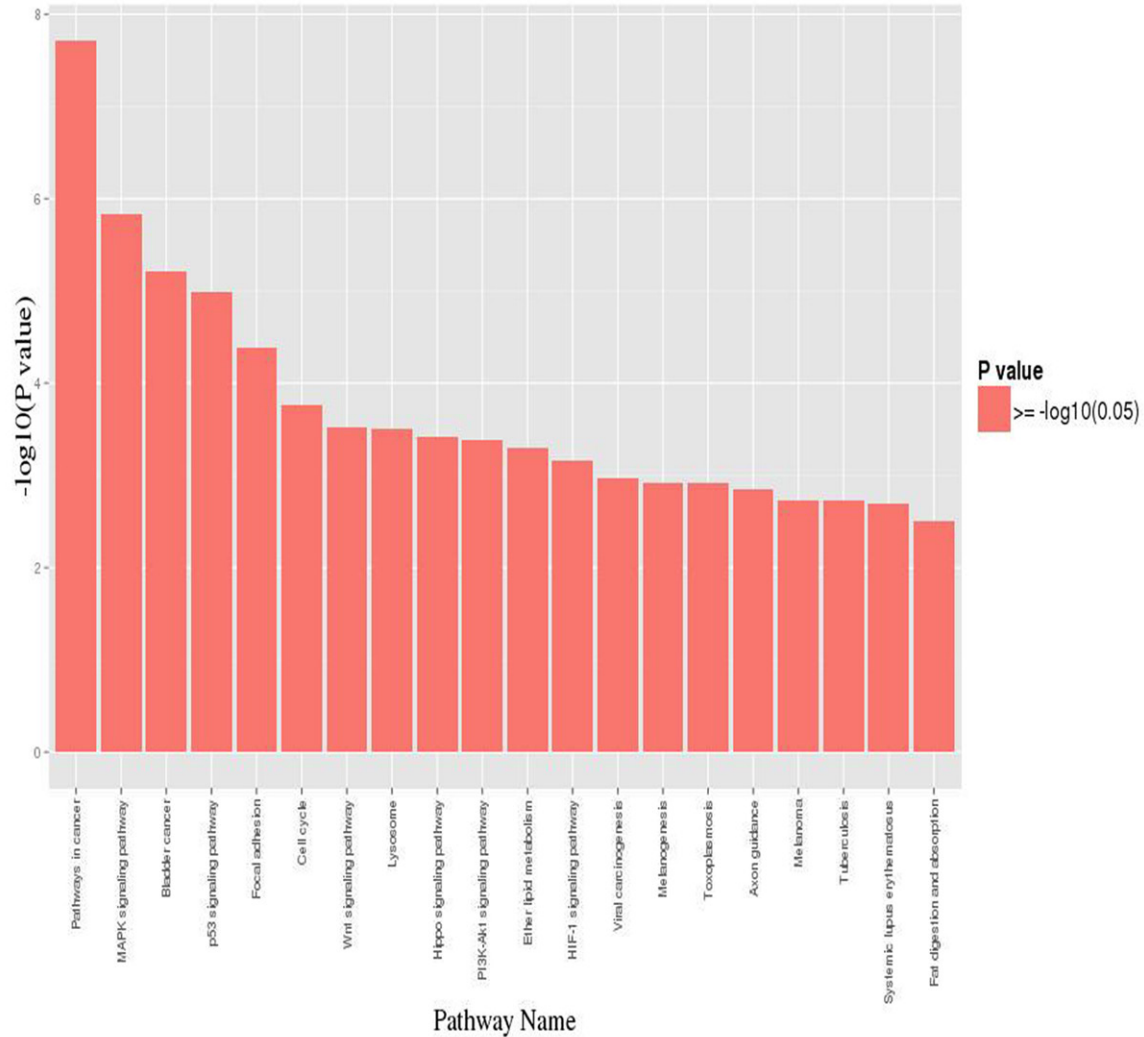


Figure 6. Function enrichment pathway of the differentially expressed genes in mEBs treated with AOB at 100 µg/ml. High concentration of AOB had negative effect on various signaling pathways.

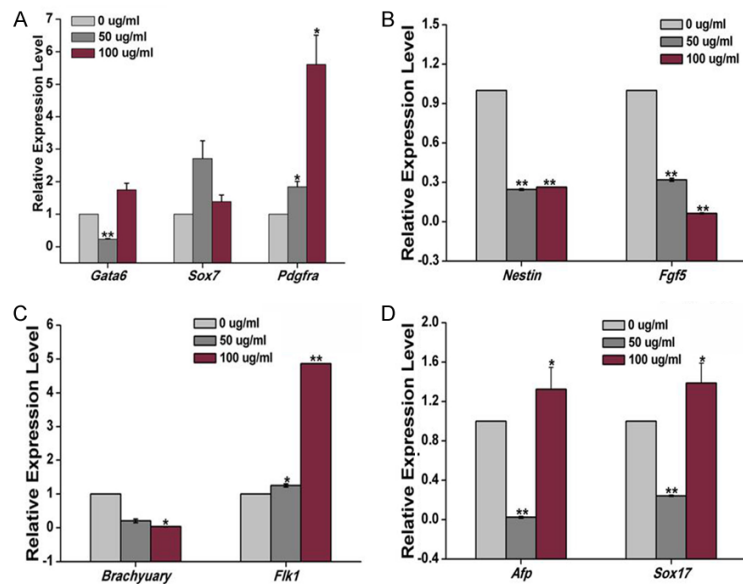


Figure 7. Real-time PCR analysis of the expression levels of the marker genes in three layers of mEBs. A: The mRNA expression levels of GATA6, SOX7, and Pdgfra in mEBs following different treatments (0 µg/ml, 50 µg/ml or 100 µg/ml AOB) were determined by real-time PCR. B: The mRNA expression levels of Nestin and FGF5 in mEBs following different treatments were determined by real-time PCR. C: The mRNA expression levels of Brachyury and Fik1 in mEBs following different treatments were determined by real-time PCR. D: The mRNA expression levels of Afp and Sox17 in mEBs following different treatments were determined by real-time PCR.

The effect of AOB on mES

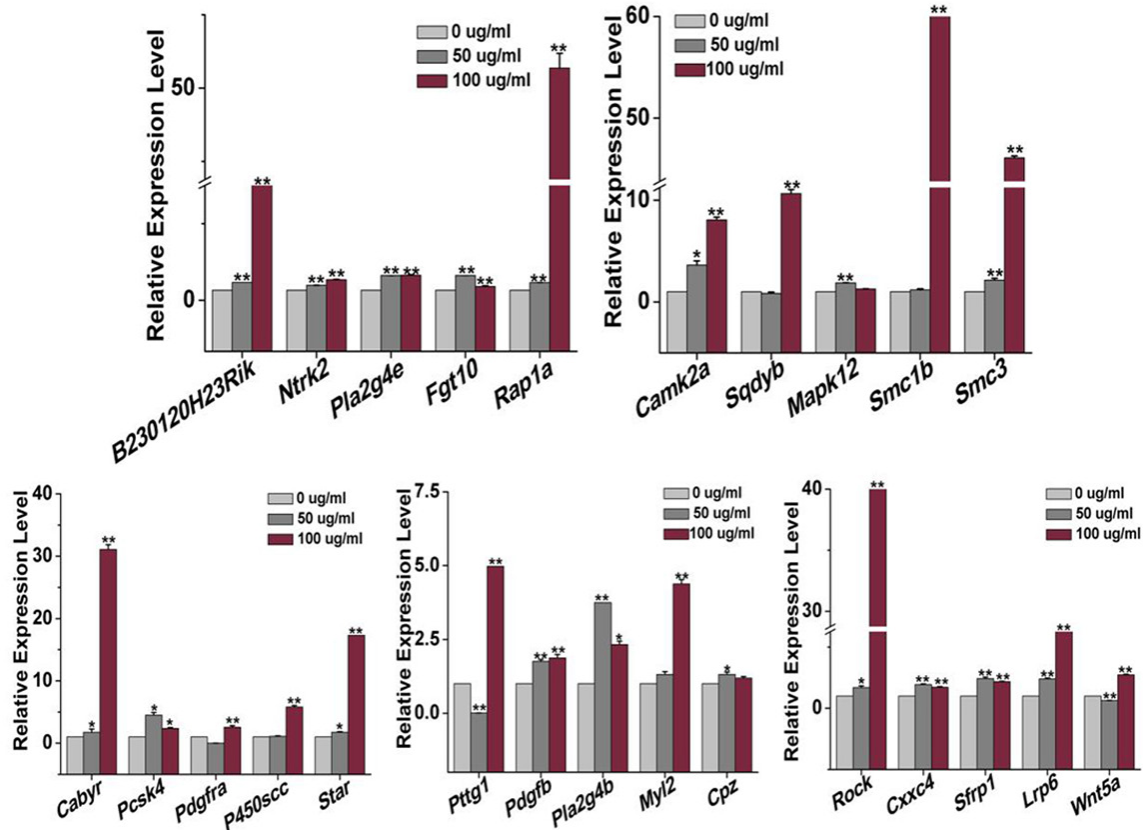


Figure 8. Real-time PCR analysis of the expression levels of reproduction-related genes in mEBs. The mRNA expression levels of reproduction-related genes in mEBs following different treatments (0 μ g/ml, 50 μ g/ml or 100 μ g/ml AOB) were determined by real-time PCR.

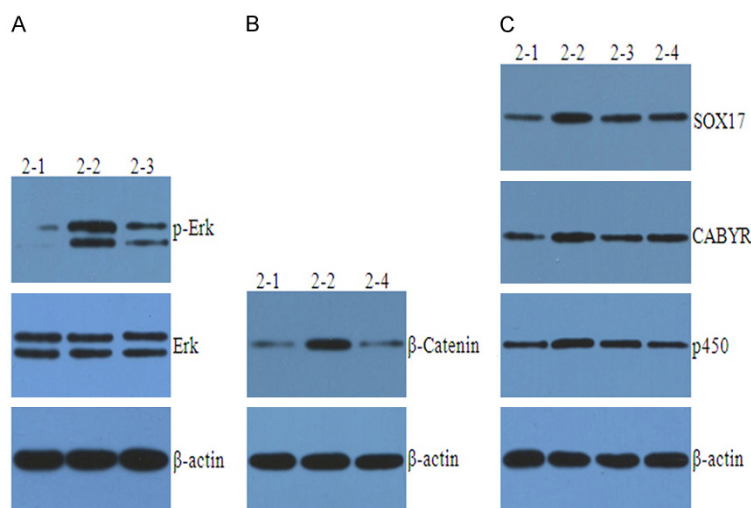


Figure 9. Western blot analysis of the protein expression levels of p-ERK, ERK, β -catenin, P450, CABYR, and SOX17 in mEBs. The levels of p-ERK, ERK (A), β -catenin (B), SOX17, P450, CABYR (C) in mEBs were determined by Western blot with the indicated antibodies. 2-1, control; 2-2, treatment with AOB alone; 2-3, treatment with AOB+U0126; 2-4, treatment with AOB+DKK1.

increased the level of p-ERK ($P < 0.01$), whereas treatment with ERK pathway inhibitor U0126 markedly depressed the level of p-ERK in AOB-treated mEBs ($P < 0.01$). Moreover, the expressions of β -catenin, SOX17, CABYR, and P450scc were significantly increased with AOB treatment but decreased both by treatment with AOB+U0126 and AOB+DKK1 (Wnt pathway inhibitor) ($P < 0.01$).

Discussions

ES cells are distinguished by their ability to differentiate into any cell type and to propagate [11-13]. Because of their plasticity and potentially un-

limited capacity for self-renewal, embryonic stem cell therapies have been proposed for regenerative medicine and tissue replacement after injury or disease [14]. EBs, differentiated from ES cells, recapitulate many aspects of cell differentiation during early embryogenesis. Self-renewal and pluripotency are the central features in defining ESC, in which Oct4 and Nanog play key roles in the maintenance of these processes [15]. Rock and Cxhc4 participate embryonic development by regulating Wnt pathways. LRP6 and Sfrp1 are crucial genes associated with regulation of reproductive function and gonadal development mediated by Wnt pathway [16, 17]. In our data, the expressions of Rock, Cxhc4, LRP6, and Sfrp1 increased significantly in AOB-treated mEBs. Wnt5a, encoded by the WNT5A gene which related to the development of uterus, has been reported to activate Wnt5a receptor (Fzd and LRP5/6) on the surface of Spermatogonial stem cells (SSCs) and then promoted Wnt pathway activation [18-20]. The interdiction of Wnt pathway may cause SSCs apoptosis. Our data showed that Wnt5a expression in the EB 50 group was significantly downregulated, but remarkably increased in the EB 100 group, as compared with the control group. These results indicated that AOB treatment had embryotoxic effects via activating Wnt signaling pathway. Furthermore, we found that the expressions of B23O120H23Rik, Pla2g4e, and Fg10, which are involved in MAPK pathway, were markedly upregulated in AOB-treated groups. This result indicated that AOB might influence the gene functions involved in reproduction and embryonic development in mouse.

In conclusion, we investigated the gene expressions related to reproduction and embryonic development in mEB and mES cells treated with different concentrations of AOB. We found that 100 µg/ml AOB treatments were more impactful on the gene expressions, compared with 50 µg/ml AOB treatment. This result indicated that the embryotoxicity of AOB relied on its concentration. Our findings suggested that AOB might enhance the activation of ERK and Wnt pathway, thus influencing the cellular processes.

Acknowledgements

The project was supported by the Research Foundation for Giant Panda Breeding of Che-

ngdu (Project Grant NO, CPF2012-15), and China Agriculture Research System (CARS-05).

Disclosure of conflict of interest

None.

Address correspondence to: Muyuan Zhu and Xiaoli Zhao, Key Laboratory for Cell and Gene Engineering of Zhejiang Province, College of Life Sciences, Zhejiang University, Hangzhou 310012, Zhejiang Province, China. E-mail: muyuanm_zhu@163.com (MYZ); zhaoxiaoli@zju.edu.cn (XLZ)

References

- [1] Lu B, Wu X, Shi J, Dong Y and Zhang Y. Toxicology and safety of antioxidant of bamboo leaves. Part 2: developmental toxicity test in rats with antioxidant of bamboo leaves. *Food Chem Toxicol* 2006; 44: 1739-1743.
- [2] Ma X, Wang E, Lu Y, Wang Y, Ou S and Yan R. Acylation of antioxidant of bamboo leaves with fatty acids by lipase and the Acylated Derivatives' efficiency in the inhibition of acrylamide formation in Fried Potato Crisps. *PLoS One* 2015; 10: e0130680.
- [3] Shi XC, Liu XQ, Xie XL, Xu YC and Zhao ZX. Gene chip array for differentiation of mycobacterial species and detection of drug resistance. *Chin Med J (Engl)* 2012; 125: 3292-3297.
- [4] Yoshimura Y, Nakamura K, Endo T, Kajitani N, Kazuki K, Kazuki Y, Kugoh H, Oshimura M and Ohbayashi T. Mouse embryonic stem cells with a multi-integrase mouse artificial chromosome for transchromosomal mouse generation. *Transgenic Res* 2015; 24: 717-727.
- [5] Banuelos CA, Banath JP, MacPhail SH, Zhao J, Eaves CA, O'Connor MD, Lansdorp PM and Olive PL. Mouse but not human embryonic stem cells are deficient in rejoining of ionizing radiation-induced DNA double-strand breaks. *DNA Repair (Amst)* 2008; 7: 1471-1483.
- [6] Ishimi Y, Abe E, Jin CH, Miyaura C, Hong MH, Oshida M, Kurosawa H, Yamaguchi Y, Tomida M, Hozumi M and et al. Leukemia inhibitory factor/differentiation-stimulating factor (LIF/D-factor): regulation of its production and possible roles in bone metabolism. *J Cell Physiol* 1992; 152: 71-78.
- [7] He Z, Li JJ, Zhen CH, Feng LY and Ding XY. Effect of leukemia inhibitory factor on embryonic stem cell differentiation: implications for supporting neuronal differentiation. *Acta Pharmacol Sin* 2006; 27: 80-90.
- [8] Desbaillets I, Ziegler U, Groscurth P and Gassmann M. Embryoid bodies: an in vitro model of mouse embryogenesis. *Exp Physiol* 2000; 85: 645-651.

- [9] Doughton G, Wei J, Tapon N, Welham MJ and Chalmers AD. Formation of a polarised primitive endoderm layer in embryoid bodies requires fgfr/erk signalling. *PLoS One* 2014; 9: e95434.
- [10] Kim PT, Hoffman BG, Plesner A, Helgason CD, Verchere CB, Chung SW, Warnock GL, Mui AL and Ong CJ. Differentiation of mouse embryonic stem cells into endoderm without embryoid body formation. *PLoS One* 2010; 5: e14146.
- [11] Laval F and Pain B. Chicken embryonic stem cells as a non-mammalian embryonic stem cell model. *Dev Growth Differ* 2010; 52: 101-114.
- [12] Morey L and Di Croce L. Analysis of endogenous protein interactions of polycomb group of proteins in mouse embryonic stem cells. *Methods Mol Biol* 2016; 1480: 153-165.
- [13] Ghanian MH, Farzaneh Z, Barzin J, Zandi M, Kazemi-Ashtiani M, Alikhani M, Ehsani M and Baharvand H. Nanotopographical control of human embryonic stem cell differentiation into definitive endoderm. *J Biomed Mater Res A* 2015; 103: 3539-3553.
- [14] Kim HK, Kim MG and Leem KH. Osteogenic activity of collagen peptide via ERK/MAPK pathway mediated boosting of collagen synthesis and its therapeutic efficacy in osteoporotic bone by back-scattered electron imaging and microarchitecture analysis. *Molecules* 2013; 18: 15474-15489.
- [15] Lee SH, Chen TY, Dhar SS, Gu B, Chen K, Kim YZ, Li W and Lee MG. A feedback loop comprising PRMT7 and miR-24-2 interplays with Oct4, Nanog, Klf4 and c-Myc to regulate stemness. *Nucleic Acids Res* 2016; 44: 10603-10618.
- [16] Bikorimana E, Lapid D, Choi H and Dahl R. Retroviral infection of murine embryonic stem cell derived embryoid body cells for analysis of hematopoietic differentiation. *J Vis Exp* 2014; e52022.
- [17] Yan YB, Li JM, Xiao E, An JG, Gan YH and Zhang Y. A pilot trial on the molecular pathophysiology of traumatic temporomandibular joint bony ankylosis in a sheep model. Part I: expression of Wnt signaling. *J Craniomaxillofac Surg* 2014; 42: e15-22.
- [18] Yeh JR, Zhang X and Nagano MC. Indirect effects of Wnt3a/beta-catenin signalling support mouse spermatogonial stem cells in vitro. *PLoS One* 2012; 7: e40002.
- [19] Yeh JR, Zhang X and Nagano MC. Wnt5a is a cell-extrinsic factor that supports self-renewal of mouse spermatogonial stem cells. *J Cell Sci* 2011; 124: 2357-2366.
- [20] Golestaneh N, Beauchamp E, Fallen S, Kokkinaki M, Uren A and Dym M. Wnt signaling promotes proliferation and stemness regulation of spermatogonial stem/progenitor cells. *Reproduction* 2009; 138: 151-162.